British Journal of Pharmacology (2004) 143, 186–192
www.nature.com/bjp

TRPM2 channel opening in response to oxidative stress is dependent on activation of poly(ADP-ribose) polymerase

*,[1,2]Elena Fonfria, [1,2]Ian C.B. Marshall, [1]Christopher D. Benham, [1]Izzy Boyfield, [1]Jason D. Brown, [1]Kerstin Hill, [1]Jane P. Hughes, [1]Stephen D. Skaper & [1]Shaun McNulty

[1]Neurology and GI Centre of Excellence for Drug Discovery, GlaxoSmithKline Research and Development Limited, New Frontiers Science Park, Third Avenue, Harlow, Essex CM19 5AW

1 TRPM2 (melastatin-like transient receptor potential 2 channel) is a nonselective cation channel that is activated under conditions of oxidative stress leading to an increase in intracellular free Ca^{2+} concentration ($[Ca^{2+}]_i$) and cell death. We investigated the role of the DNA repair enzyme poly(ADP-ribose) polymerase (PARP) on hydrogen peroxide (H_2O_2)-mediated TRPM2 activation using a tetracycline-inducible TRPM2-expressing cell line.

2 In whole-cell patch-clamp recordings, intracellular adenine 5′-diphosphoribose (ADP-ribose) triggered an inward current in tetracycline-induced TRPM2-human embryonic kidney (HEK293) cells, but not in uninduced cells. Similarly, H_2O_2 stimulated an increase in $[Ca^{2+}]_i$ (pEC_{50} 4.54 ± 0.02) in Fluo-4-loaded TRPM2-expressing HEK293 cells, but not in uninduced cells. Induction of TRPM2 expression caused an increase in susceptibility to plasma membrane damage and mitochondrial dysfunction in response to H_2O_2. These data demonstrate functional expression of TRPM2 following tetracycline induction in TRPM2-HEK293 cells.

3 PARP inhibitors SB750139-B (patent number DE10039610-A1 (Lubisch *et al*., 2001)), PJ34 (*N*-(6-oxo-5,6-dihydro-phenanthridin-2-yl)-*N*,*N*-dimethylacetamide) and DPQ (3, 4-dihydro-5-[4-(1-piperidinyl)butoxy]-1(2H)-isoquinolinone) inhibited H_2O_2-mediated increases in $[Ca^{2+}]_i$ (pIC_{50} vs 100 μM H_2O_2: 7.64 ± 0.38; 6.68 ± 0.28; 4.78 ± 0.05, respectively), increases in mitochondrial dysfunction (pIC_{50} vs 300 μM H_2O_2: 7.32 ± 0.23; 6.69 ± 0.22; 5.44 ± 0.09, respectively) and decreases in plasma membrane integrity (pIC_{50} vs 300 μM H_2O_2: 7.45 ± 0.27; 6.35 ± 0.18; 5.29 ± 0.12, respectively). The order of potency of the PARP inhibitors in these assays (SB750139 > PJ34 > DPQ) was the same as for inhibition of isolated PARP enzyme.

4 SB750139-B, PJ34 and DPQ had no effect on inward currents elicited by intracellular ADP-ribose in tetracycline-induced TRPM2-HEK293 cells, suggesting that PARP inhibitors are not interacting directly with the channel.

5 SB750139-B, PJ34 and DPQ inhibited increases in $[Ca^{2+}]_i$ in a rat insulinoma cell line (CRI-G1 cells) endogenously expressing TRPM2 (pIC_{50} vs 100 μM H_2O_2: 7.64 ± 0.38; 6.68 ± 0.28; 4.78 ± 0.05, respectively).

6 These data suggest that oxidative stress causes TRPM2 channel opening in both recombinant and endogenously expressing cell systems *via* activation of PARP enzymes.
British Journal of Pharmacology (2004) **143,** 186–192. doi:10.1038/sj.bjp.0705914

Keywords: TRPM2; hydrogen peroxide; PARP; oxidative stress; SB750139-B; PJ34; DPQ; CRI-G1

Abbreviations: ADP-ribose, adenine 5′-diphosphoribose; $[Ca^{2+}]_i$, intracellular free calcium ion concentration; DPQ, 3, 4-dihydro-5-[4-(1-piperidinyl)butoxy]-1(2H)-isoquinolinone; FCCP, carbonyl cyanide 4 (trifluoromethoxy) phenylhydrazone; H_2O_2, hydrogen peroxide; NAD, nicotinamide adenine dinucleotide; PARP, poly(ADP-ribose) polymerase; PJ34, *N*-(6-oxo-5,6-dihydro-phenanthridin-2-yl)-*N*,*N*-dimethylacetamide; SB750139-B, patent number DE10039610-A1 (Lubisch *et al*., 2001); TRPM2, melastatin-like transient receptor potential 2 channel

Introduction

TRPM2 (melastatin-like transient receptor potential 2), formerly known as TRPC7 and LTRPC2, is a nonselective cation channel highly expressed in the brain (Nagamine *et al*., 1998; Hara *et al*., 2002; Kraft *et al*., 2004) and in immune cells (Perraud *et al*., 2001; Sano *et al*., 2001) that is thought to respond to changes in oxidative stress (Hara *et al*., 2002; Wehage *et al*., 2002). TRPM2 activation has been demonstrated upon extracellular application of oxidants such as hydrogen peroxide (H_2O_2), tertbutylhydroperoxide and dithionite (Hara *et al*., 2002; Wehage *et al*., 2002), the second messenger arachidonic acid (Hara *et al*., 2002), intracellular application of adenine 5′-diphosphoribose (ADP-ribose) or nicotinamide adenine dinucleotide (NAD) (Perraud *et al*., 2001; Sano *et al*., 2001; Hara *et al*., 2002; Wehage *et al*., 2002; Inamura *et al*., 2003; McHugh *et al*., 2003). Once activated, TRPM2 causes a sustained elevation in intracellular free calcium ion concentration ($[Ca^{2+}]_i$) and subsequent cell death (Hara *et al*., 2002; Zhang *et al*., 2003). To date, the molecular

*Author for correspondence; Email: Elena.2.Fonfria@gsk.com
[2]Both these authors contributed equally to this work
Advance online publication: 9 August 2004

links between oxidative stress and TRPM2 activation have not been described.

ADP-ribose has emerged as a strong candidate for the endogenous activator of TRPM2. Intracellular application of ADP-ribose activates TRPM2 channels in whole-cell patch-clamp experiments (Perraud *et al*., 2001; Sano *et al*., 2001; Hara *et al*., 2002; Wehage *et al*., 2002; Inamura *et al*., 2003; McHugh *et al*., 2003) independent of immediate breakdown products of ADP-ribose (Perraud *et al*., 2001). Furthermore, TRPM2 possesses a Nudix hydrolase domain on the C-terminus that functions as a specific ADP-ribose pyrophosphatase (Perraud *et al*., 2001). Both a deletion mutant (Hara *et al*., 2002) and splice variant (Zhang *et al*., 2003) lacking this domain have demonstrated compromised activation in response to oxidative stress. Curiously, a neutrophil TRPM2 splice variant lacking the ADP-ribose pyrophosphatase domain is reported to show H_2O_2-mediated activation (Wehage *et al*., 2002). In the same way, Heiner *et al*. (2003) reported a deletion mutant lacking part of the C-terminus upstream of the Nudix motif in which H_2O_2, but not ADP-ribose, mediates activation of TRPM2 (Heiner *et al*., 2003). These results suggest that the mechanism of TRPM2 activation may not be universal.

In the present study, we considered the role of poly(ADP-ribose) polymerase (PARP) enzymes as a potential source of ADP-ribose for the activation of TRPM2 under conditions of oxidative stress. PARP-1, the most abundant of the PARP family, is a nuclear enzyme that binds to single- and double-stranded DNA breaks resulting from various toxic stimuli including oxidants, alkylating agents and ionising radiation (Virag & Szabo, 2002). Once bound, PARP-1 catalyses the cleavage of NAD into nicotinamide and ADP-ribose and polymerises ADP-ribose onto various nuclear proteins, including histones and transcription factors, resulting in the activation of DNA repair mechanisms and stimulation of nuclear factor κB-mediated transcription (Tanuma *et al*., 1985; de Murcia & Menissier, 1994; Oliver *et al*., 1999; Virag & Szabo, 2002). Under conditions of severe oxidative stress, PARP-1 becomes overactivated leading to consumption of NAD and ATP and ultimately cellular dysfunction and cell death.

Here, we present evidence for a direct role of PARP enzymes in linking oxidative stress with TRPM2 activation in both a recombinant cell system and in a rat insulinoma cell line, CRI-G1, endogenously expressing TRPM2.

Experimental procedures

Cell culture

Human embryonic kidney (HEK293) cells expressing tetracycline-inducible human Flag-tagged TRPM2 (TRPM2-HEK293 cells) grown in minimum essential medium (MEM) supplemented with nonessential amino acids, 10% foetal calf serum and 0.2 mM L-glutamine were maintained under 5% CO_2 at 37°C. TRPM2 expression was induced by incubating cells for 24 h with 1 μg ml^{-1} tetracycline (Perraud *et al*., 2001). Rat insulinoma CRI-G1 cells (ECACC Clone Ref. no. 87052701) endogenously expressing TRPM2 were cultured in Dulbecco's minimum essential medium (DMEM) supplemented with 10% foetal calf serum and 2 mM L-glutamine and maintained under 5% CO_2 at 37°C. All cell culture media were obtained from Invitrogen (Paisley, U.K.). For Ca^{2+} and cell death analysis, TRPM2-HEK293 and CRI-G1 cells were seeded into black-walled, clear-bottom 96-well plates (Costar, U.K.) at a density of 25,000–30,000 cells well^{-1} and incubated at 37°C/5% CO_2 overnight.

Measurement of $[Ca^{2+}]_i$ using a fluorometric imaging plate reader (FLIPR)

TRPM2-HEK293 or CRI-G1 cells were loaded with 4 μM Fluo-4 AM (Teflabs, Austin, U.S.A.) at 22°C for 1 h, washed with Ca^{2+}-free Tyrodes medium (mM: NaCl 145, KCl 2.5, HEPES 10, glucose 10, $MgCl_2$ 1.2, ethylene glycol-bis(β-aminoethyl ether)-*N*,*N*,*N*′,*N*′-tetraacetic acid (EGTA) 1, pH 7.4) in order to remove extracellular Fluo-4 AM and incubated for a further 30 min at room temperature. Fluorescence ($\lambda_{ex} = 488$ nm, $\lambda_{em} = 540$ nm) from each well was measured using a FLIPR (Molecular Devices, U.K.) before and after the addition of H_2O_2 and 2 mM Ca^{2+}. Three independent experiments were generated using 10 concentrations of H_2O_2 in quadruplicate. For experiments involving mitochondrial uncoupling, carbonylcyanide-4-(trifluoromethoxy)phenylhydrazone (FCCP, Sigma-Aldrich, Dorset, U.K.) was added in place of H_2O_2. For experiments involving PARP inhibitors, cells were preincubated for 30 min with SB750139-B (patent number DE10039610-A1 (Lubisch *et al*., 2001)), PJ34 (*N*-(6-oxo-5,6-dihydro-phenanthridin-2-yl)-*N*,*N*-dimethylacetamide) or DPQ (3, 4-dihydro-5-[4-(1-piperidinyl) butoxy]-1(2H)-isoquinolinone) prior to the addition of H_2O_2. SB750139-B and PJ34 were synthesised in-house by standard chemical procedures and DPQ was purchased from Calbiochem, Nottingham, U.K.

Cell death assays

Measurement of plasma membrane integrity using Sytox Green TRPM2-HEK293 or CRI-G1 cells were rinsed and incubated with fresh Ca^{2+}-containing growth medium containing 1 μM Sytox Green (Molecular Probes, Eugene, OR, U.S.A.) and H_2O_2 as indicated. For experiments involving PARP inhibitors, cells were preincubated for 1 h with test compound prior to the addition of H_2O_2. Sytox Green fluorescence ($\lambda_{ex} = 485$ nm, $\lambda_{em} = 525$ nm) from each well was measured using a FLEXStation (Molecular Devices, Wokingham, U.K.). Three independent experiments were generated for DPQ, SB750139-B and PJ34 in the presence of H_2O_2 using seven concentrations in triplicate. Data were expressed as arbitrary fluorescence units or % Sytox Green fluorescence (100 × fluorescence emission in the presence of PARP inhibitor/fluorescence emission in the absence of PARP inhibitor).

MTT cell viability assay TRPM2-HEK293 or CRI-G1 cells were rinsed and incubated with fresh Ca^{2+}-containing growth media. For experiments involving PARP inhibitors, cells were preincubated for 1 h with test compound prior to the addition of 300 μM H_2O_2. After 20 h, the MTT assay was performed using the Cell Titer 96 nonradioactive proliferation assay according to the manufacturer's instructions (Promega, Southampton, U.K.). Three independent experiments were performed for DPQ, SB750139-B and PJ34 using seven concentrations in triplicate. Data were expressed as the percent

of metabolic activity (well fluorescence − blank) × 100/(control well fluorescence − blank).

PARP enzymatic activity assay

Enzyme velocities were quantified by a scintillation proximity assay in 96-well plate format using a human PARP-1–glutathione-*S*-transferase fusion protein. The reaction mix contained 6 nM PARP-1 enzyme, 1.5 μg ml^{-1} activated calf thymus DNA, 3 μM cold NAD and [^{3}H]-NAD (3.3 μCi−well^{-1}; Perkin-Elmer Life Sciences, U.K.). After 10 min incubation at room temperature, the reaction was terminated by adding stop solution (5 mg ml^{-1} glutathione-coated yttrium silicate scintillation proximity assay beads, Amersham Pharmacia, U.K.; 100 μM benzamide; 20 mM EDTA). The plates were sealed and shaken before analysis in a 1450 Micro-Beta Plus Counter (Wallac, U.K.). The 10-point experiments were performed in duplicate.

Western blot analysis of TRPM2 expression

Protein in each whole-cell lysate from TRPM2-HEK293 cells was quantified (Bio-Rad, Hemel Hempstead, U.K.) and 25 μg of protein was electroblotted. Following blotting, membranes were incubated with anti-Flag antibody diluted 1 : 10,000 (Sigma-Aldrich, Dorset, U.K.), washed and incubated with a horseradish peroxidase-conjugated secondary antibody (1 : 5000 dilution; Amersham Pharmacia, U.K.). ECL was used for detection of signal (Perbio Science U.K. Limited, Chester, U.K.).

Electrophysiological analysis of TRPM2 expression

Experiments were performed at room temperature using whole-cell voltage-clamp recording mode. Electrodes were pulled from borosilicate glass capillaries and typically had a resistance of 2–4 MΩ for the whole-cell experiments. Recordings were made using an Axopatch 200B patch-clamp amplifier (Axon Instruments Inc., U.S.A.). Data were recorded on a PC using PCLAMP 8 software (Axon Instruments Inc., U.S.A.). In the whole-cell mode, the cell was clamped to −50 mV. The extracellular solution consisted of 140 mM NaCl, 5 mM KCl, 2 mM $MgCl_2$, 1 mM $CaCl_2$, 10 mM HEPES (pH 7.3) for the Ca^{2+}-containing solution, and 140 mM NaCl, 5 mM KCl, 2 mM $MgCl_2$, 1 mM $BaCl_2$, 10 mM HEPES (pH 7.3) for the Ca^{2+}-free solution (pH was adjusted with NaOH). Patch pipettes were filled with the following solutions: 120 mM K^+ gluconate, 10 mM KCl, 2 mM $MgCl_2$, 10 mM HEPES (pH 7.3) (adjusted with KOH). TRPM2 channels were activated by adding ADP-ribose to a concentration of 0.1 mM to the intracellular recording solution. Cells typically had a capacitance of 17 ± 1 pF. Series resistance was typically 5–7 MΩ and was not compensated. It is acknowledged that the lack of series resistance compensation may have resulted in substantial errors in reported holding potential, although these would not be anticipated to impact upon the relative differences between data in the presence and absence of PARP inhibitors. During recordings, cells were usually voltage clamped at −50 mV and perfused from a rapid solution exchange device. This equipment permitted complete solution exchanges to be made in < 100 ms. In all experiments, membrane current was filtered at 2 kHz (four-pole Bessel characteristic filter) and sampled continuously at 5 kHz. For analysing the effect of PARP inhibitors, the cells were preincubated in 10 μM PARP inhibitor for 1–2 h at 37°C in normal cell culture buffer and were transferred for the patch-clamp experiments to extracellular solution containing 10 μM of the corresponding PARP inhibitor.

Data analysis

Data were expressed as mean ± s.e. The computer program GraphPad Prism (GraphPad Software Inc., San Diego, U.S.A.) was used for curve fitting and statistical analysis.

Results

TRPM2 expression on HEK293 cells and CRI-G1 cells

Tetracycline (1 μg ml^{-1}, 24 h) induced a robust expression of TRPM2 in the tetracycline-inducible HEK-293 Flag-TRPM2 cell line. A 170 kDa band corresponding to Flag-tagged TRPM2 protein was identified in cell lysates from tetracycline-induced TRPM2-HEK293 by using an anti-Flag antibody (Figure 1a). The apparent molecular weight of 170 kDa is in agreement with the Flag-tagged TRPM2 reported previously (Perraud *et al*., 2001; McHugh *et al*., 2003). Immunostaining was not evident in noninduced cells. TRPM2 was endogenously expressed by the rat insulinoma cell line CRI-G1 (Inamura *et al*., 2003) as confirmed by quantitative RT–PCR (data not shown).

H_2O_2 and ADP-ribose trigger activation of TRPM2

In whole-cell patch-clamp experiments, intracellular application of ADP-ribose triggered a calcium-dependent cation current in tetracycline-induced TRPM2-expressing HEK293 cells (Figure 1b) and in CRI-G1 cells (Figure 1c). The values for the current densities for the induced TRPM2-HEK293 cells were 5 ± 1 pA pF^{-1} (−50 mV holding potential) in the absence of ADP-ribose and 340 ± 21 pA pF^{-1} in the presence of 100 μM ADP-ribose in the patch pipette. Noninduced TRPM2-HEK293 cells showed a current density of 2 ± 1 pA pF^{-1} (−50 mV holding potential) in the absence of intracellular ADP-ribose. Similarly, H_2O_2 triggered an increase in Fluo-4 fluorescence in both induced TRPM2-HEK293 cells (pEC_{50} 4.54 ± 0.02, $n = 4$, Figure 2a) and in CRI-G1 cells (pEC_{50} 4.08 ± 0.12, $n = 3$, data not shown) indicative of a rise in $[Ca^{2+}]_i$. H_2O_2 did not produce any significant increase in $[Ca^{2+}]_i$ in uninduced TRPM2-HEK293 cells (Figure 2a).

Consistent with the reported activity of TRPM2 as a cell death channel (Hara *et al*., 2002; Zhang *et al*., 2003), a heightened sensitivity to oxidative stress-mediated cell death was evident in TRPM2-expressing cells compared to non-induced cells. Plasma membrane integrity (Sytox Green assay) was significantly compromised in tetracycline-induced TRPM2-HEK293 cells after 5–20 h exposure to 300 μM H_2O_2 compared to noninduced cells (Figure 2b). Similarly, tetracycline-induced TRPM2-HEK293 cells exposed to 300 μM H_2O_2 for 18 h showed a significantly greater loss of metabolic activity compared to noninduced cells as determined by MTT (Figure 2c).

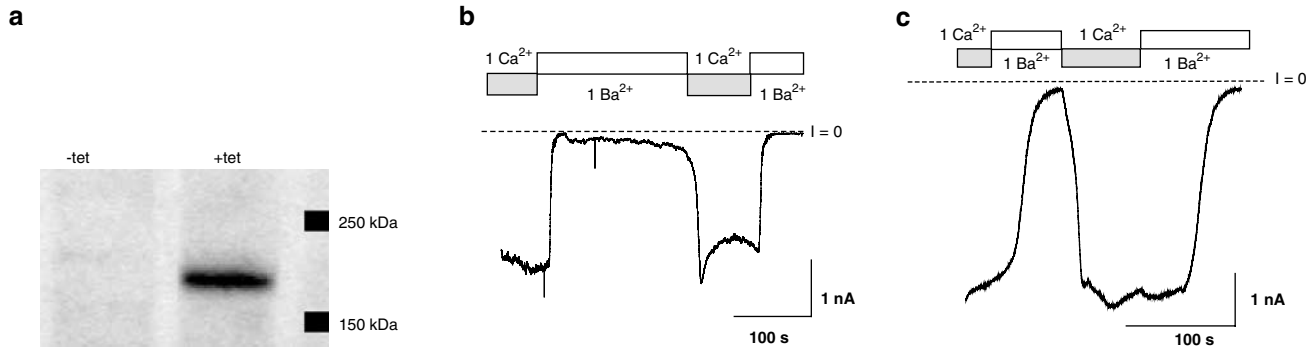

Figure 1 Functional expression of TRPM2 in tetracycline-inducible TRPM2-HEK293 cells and in CRI-G1 cells. (a) Western blot of induced (+tet) and uninduced (−tet) TRPM2-HEK293 cells. Immunodetection of the Flag epitope revealed the expression of the TRPM2-Flag construct on the induced cells. TRPM2 currents activated by intracellular ADP-ribose in TRPM2-HEK293 cells (b) and CRI-G1 cells (c) are reversibly blocked by exchange of 1 mM extracellular Ca^{2+} (1 Ca^{2+}) with 1 mM Ba^{2+} (1 Ba^{2+}). Whole-cell patch-clamp recordings were conducted with 100 μM ADP-ribose present in the patch pipette and typical whole-cell currents are shown at −50 mV.

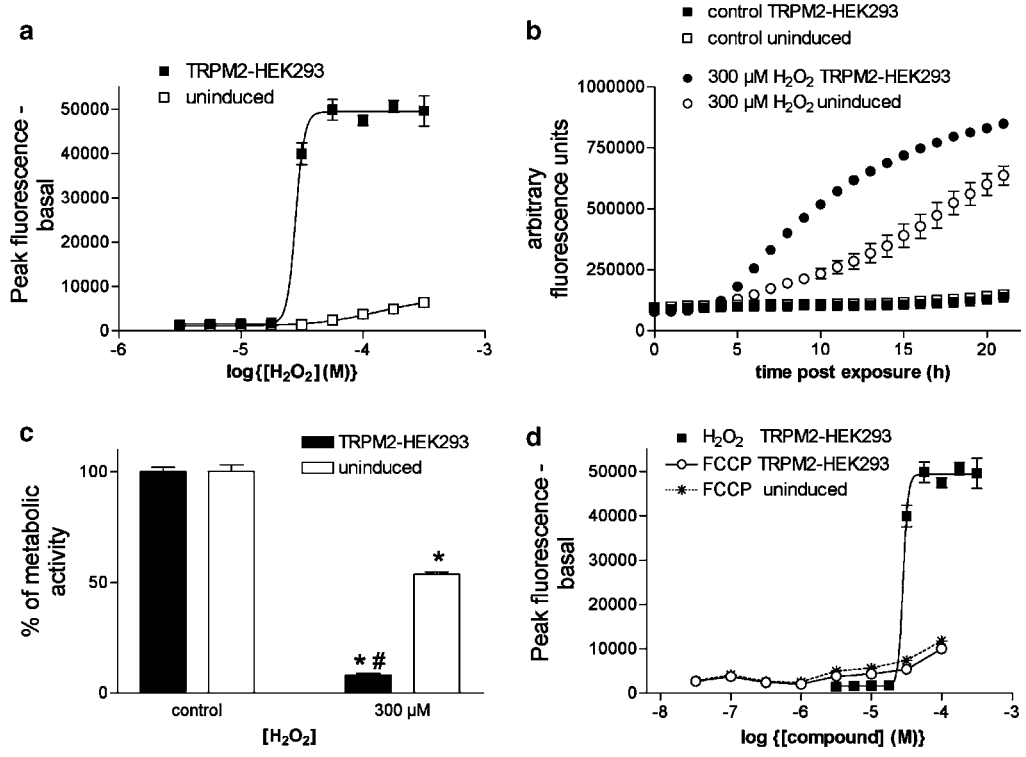

Figure 2 TRPM2 expression in TRPM2-HEK293 cells confers sensitivity to H_2O_2. (a) $[Ca^{2+}]_i$ rise in response to H_2O_2. (b) H_2O_2-induced loss of cell membrane integrity as assessed by Sytox Green incorporation. (c) Loss of metabolic activity in response to 300 μM H_2O_2, as assessed by the MTT assay. $^*P<0.001$ vs respective control; $^{\#}P<0.001$ vs uninduced cells (one-way ANOVA followed by Tukey's post-test). (d) $[Ca^{2+}]_i$ rise in response to FCCP. One representative experiment is shown. Similar results were obtained in three to four independent experiments.

The mitochondrial uncoupler FCCP was tested to determine whether oxidative stress-dependent mitochondrial dysfunction occurred upstream of TRPM2 activation. At concentrations sufficient to induce uncoupling of mitochondria, FCCP induced only a small rise in $[Ca^{2+}]_i$ that was similar in tetracycline-induced and uninduced cells (Figure 2d). This suggests that TRPM2 activation is not a downstream consequence of mitochondrial uncoupling.

PARP inhibitors suppress H_2O_2-mediated activation of TRPM2

The effects of three structurally distinct PARP inhibitors on H_2O_2-induced $[Ca^{2+}]_i$ elevations and cell death in TRPM2-expressing HEK293 cells were investigated. PJ34, SB750139-B and DPQ inhibited the H_2O_2-mediated rise in $[Ca^{2+}]_i$ in a concentration-dependent manner (Figure 3a, Table 1) and

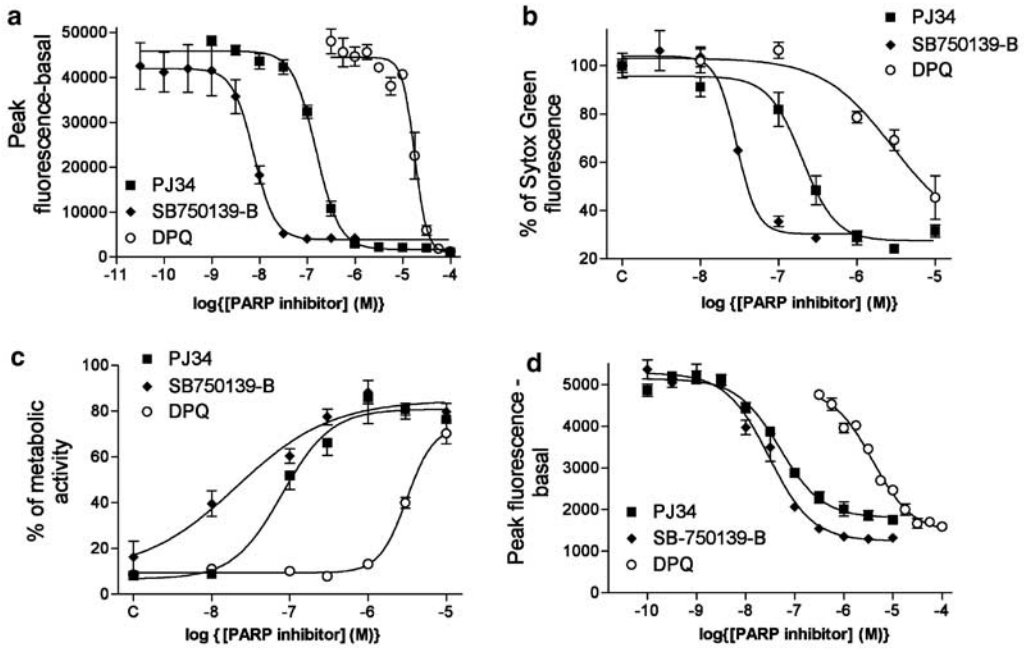

Figure 3 Effect of PARP inhibitors on TRPM2 activation and TRPM2-mediated cell death. (a) PARP inhibitors suppress 100 μM H_2O_2-induced $[Ca^{2+}]_i$ rises in TRPM2-HEK293 cells. Data are expressed as peak fluorescence minus basal. (b) PARP inhibitors suppress 300 μM H_2O_2-mediated cell membrane damage as assessed by Sytox Green incorporation in TRPM2-HEK293 cells. Data are expressed as the percent of Sytox Green fluorescence. (c) PARP inhibitors suppress H_2O_2-mediated loss of metabolic activity as assessed by the MTT assay in TRPM2-HEK293 cells. Data are expressed as the percent of metabolic activity in the absence of 300 μM H_2O_2. (d) PARP inhibitors suppress 100 μM H_2O_2-induced $[Ca^{2+}]_i$ rises in CRI-G1 cells. Data are expressed as peak fluorescence minus basal. One representative experiment is shown. Similar results were obtained in at least three independent experiments.

Table 1 Summary of the effects of the PARP inhibitors in TRPM2-HEK293 and CRI-G1 cells

PARP inhibitor	*Isolated enzyme pIC_{50} PARP activity*	*pIC_{50} Ca^{2+} response (FLIPR)*	*TRPM2-HEK293 cells pIC_{50} cell death (Sytox Green)*	*pIC_{50} cell death (MTT assay)*	*CRI-G1 cells pIC_{50} Ca^{2+} response (FLIPR)*
SB750139-B	8.7±0.1	7.6±0.4	7.5±0.3	7.3±0.2	7.4±0.1
PJ34	8.1±0. 1	6.7±0.3	6.4±0.2	6.7±0.2	7.4±0.1
DPQ	40 nM[a]	4.8±0.1	5.3±0.1	5.4±0.1	5.5±0.04

Data are means±s.e., $n=3$–7 experiments. pIC_{50} values were obtained vs 100 μM H_2O_2 for FLIPR assays and 300 μM H_2O_2 for Sytox Green and MTT assays.
[a]Eliasson *et al.* (1997). Two-way ANOVA of pIC_{50} values revealed statistically significant differences on the compounds used ($F(2,8)=42.55$, $P<0.0001$) and on the assays performed ($F(4,8)=12.39$, $P=0.002$). No statistically significant differences were found among the cellular assays ($F(3,6)=1.113$, $P=0.41$).

significantly reduced H_2O_2-induced cell death as determined by cell membrane integrity (Figure 3b, Table 1) and by mitochondrial dysfunction (Figure 3c, Table 1). In the CRI-G1 insulinoma cell line endogenously expressing TRPM2, PARP inhibitors also inhibited H_2O_2-induced rises in $[Ca^{2+}]_i$ (Figure 3d, Table 1). In all of these assays, the rank order of potency of the three PARP inhibitors (SB750139-B > PJ34 > DPQ) was the same as for inhibition of isolated PARP enzyme activity (Table 1). The higher potency of the PARP inhibitors on inhibition of isolated PARP compared to inhibition of cellular responses is probably due to limited access of the compounds to the cell interior. No statistically significant difference was found between the inhibition of H_2O_2-mediated increases in $[Ca^{2+}]_i$ in TRPM2-HEK293 cells and CRI-G1 cells ($F(1,2)=1.85$, $P=0.31$, Table 1).

Although the rank order of potency of the PARP inhibitors is consistent with their acting *via* inhibition of PARP, we tested the possibility that they interact directly with TRPM2 to block ADP-ribose-mediated channel opening. In TRPM2-HEK293 cells, the currents evoked by a submaximal concentration of ADP-ribose (100 μM) were not significantly different ($P=0.43$) following preincubation with supramaximal (10 μM) concentrations of the PARP inhibitors (mean currents±s.e: 5.4±0.43, 5.7±0.37, 6.3±0.70 and 6.38±0.57 nA for cells treated with vehicle, SB750139-B, PJ34 and DPQ, respectively). This suggests that PARP inhibitors do not have a direct

blocking action on TRPM2 channels, either by blocking ADP-ribose-mediated activation or by a direct block of the channel pore.

Discussion

Extracellular application of oxidants (Hara *et al*., 2002; Wehage *et al*., 2002) and intracellular application of ADP and NAD (Perraud *et al*., 2001; Sano *et al*., 2001; Hara *et al*., 2002; Wehage *et al*., 2002) have been shown to cause activation of TRPM2 channels in a number of systems. Our current data suggest a link between TRPM2 activation and activation of PARP enzymes. In HEK293 cells inducibly expressing TRPM2, we have shown that three structurally distinct PARP inhibitors (Lubisch *et al*., 2001; Cosi, 2002) block TRPM2-dependent increases in $[Ca^{2+}]_i$ and cell death mediated by H_2O_2 with a similar rank order of potency as for inhibition of isolated PARP. A direct action of the PARP inhibitors on TRPM2 was precluded by electrophysiological studies using ADP-ribose to activate TRPM2 directly. These results provide evidence that oxidative stress-dependent activation of TRPM2 requires PARP enzyme activity. Our use of a tetracycline-inducible TRPM2-expressing cell line to elucidate the role of PARP in peroxide-mediated TRPM2 activation raises an important question as to whether a similar pathway of activation is present in cells expressing TRPM2 endogenous levels of TRPM2. We have shown here that peroxide-mediated Ca^{2+} elevations in a rat insulinoma cell line (CRI-G1) known to express TRPM2 show a similar sensitivity to PARP inhibitors as described for TRPM2-expressing HEK293 cells. PARP activation may therefore be a key step in the activation of TRPM2 in a variety of systems.

PARP-1, the most abundant of the PARP enzyme family, has a number of key characteristics that support its role as a mediator between oxidative damage and TRPM2 activation. PARP-1 binds to single- and double-strand breaks on DNA caused by oxidative damage and catalyses the breakdown of NAD into nicotinamide and ADP-ribose. PARP-1 polymerises ADP-ribose monomers onto various nuclear proteins, including histones and transcription factors leading to initiation of DNA repair mechanisms and stimulation of nuclear factor κB-mediated transcription (Tanuma *et al*., 1985; de Murcia & Menissier, 1994; Oliver *et al*., 1999; Virag & Szabo, 2002). Free ADP-ribose, a known activator of TRPM2 (Perraud *et al*., 2001; Sano *et al*., 2001; Hara *et al*., 2002; Wehage *et al*., 2002; Inamura *et al*., 2003; McHugh *et al*., 2003), is generated following degradation of poly(ADP-ribose) polymers by poly(ADP-ribose)glycohydrolase and ADP ribosyl protein lyase activities (Virag & Szabo, 2002) and potentially as a direct consequence of NAD breakdown. Our hypothesis that free ADP-ribose generated in response to PARP activation is the physiological activator of TRPM2 relies on free ADP-ribose achieving intracellular concentrations in the range of 100 μM. Unfortunately, accurate measurements of free intracellular ADP-ribose levels following PARP activation are not reported, possibly due to difficulties associated with hydrolysis of pyridine nucleotides on extraction. However, complex subcellular localisations and novel functions have been reported for PARP-1 and related enzymes (Smith, 2001), raising the possibility that microdomains of high ADP-ribose concentration may be achieved in specific subcellular regions.

While our current data support a role for PARP enzyme activity in TRPM2-mediated responses to oxidants in certain cell types, this may not be an exclusive mechanism for TRPM2 activation. Arachidonic acid has been proposed to activate TRPM2 *via* a specific binding domain on the channel, the deletion of which causes abrogation of TRPM2-mediated responses (Hara *et al*., 2002). Furthermore, both increased intracellular Ca^{2+} (Perraud *et al*., 2001; Sano *et al*., 2001; Hara *et al*., 2002) and decreased intracellular ATP (Sano *et al*., 2001) have been reported to potentiate TRPM2 channel activity, raising the possibility that changes in Ca^{2+} or ATP levels within cells may act as the trigger for TRPM2 activation in the presence of maintained levels of ADP-ribose. However, the relationship between oxidative stress-mediated cell dysfunction and decreased ATP levels is neither clear (Kourie, 1998) nor is it known how PARP inhibitors might influence these processes. In pulmonary endothelial cells, iron chelators and xanthine oxidase inhibitors prevented H_2O_2-mediated cytotoxicity, but did not have any effect on decreased ATP levels (Varani *et al*., 1990). On the other hand, mitochondrial uncoupling by FCCP did not significantly affect $[Ca^{2+}]_i$ in TRPM2-HEK293, suggesting that ATP depletion alone does not activate TRPM2 in these cells.

In conclusion, our data support the hypothesis that PARP enzyme activity is a central component of the pathway linking oxidative stress with TRPM2 activation, and raises the question as to whether TRPM2 activation contributes to a number of pathophysiological conditions in which PARP enzyme activity has been implicated (Eliasson *et al*., 1997; Takahashi *et al*., 1997; Burkart *et al*., 1999; Skaper, 2003; Suarez-Pinzon *et al*., 2003). TRPM2 may therefore be an attractive therapeutic target for specific necrotic conditions without the liabilities associated with targeting PARP activity.

Elena Fonfria and Kerstin Hill are in receipt of an EU Framework V Postdoctoral Fellowship project MCFH-2001-00746. We thank Dr A.M. Scharenberg and Dr R.E. Kelsell for their helpful comments on the manuscript, Dr A.M. Scharenberg for the kind provision of the TRPM2-HEK293 cells and Dr C. Davis and Professor A. Randall for their assistance in the electrophysiological studies.

References

BURKART, V., WANG, Z.Q., RADONS, J., HELLER, B., HERCEG, Z., STINGL, L., WAGNER, E.F. & KOLB, H. (1999). Mice lacking the poly(ADP-ribose) polymerase gene are resistant to pancreatic beta-cell destruction and diabetes development induced by streptozocin. *Nat. Med.,* **5,** 314–319.

COSI, C. (2002). New inhibitors of poly(ADP-ribose) polymerase and their potential therapeutic targets. *Expert Opin. Ther. Patents,* **12,** 1047–1071.

DE MURCIA, G. & MENISSIER, D.M. (1994). Poly(ADP-ribose) polymerase: a molecular nick-sensor. *Trends Biochem. Sci.,* **19,** 172–176.

ELIASSON, M.J., SAMPEI, K., MANDIR, A.S., HURN, P.D., TRAYSTMAN, R.J., BAO, J., PIEPER, A., WANG, Z.Q., DAWSON, T.M., SNYDER, S.H. & DAWSON, V.L. (1997). Poly(ADP-ribose) polymerase gene disruption renders mice resistant to cerebral ischemia. *Nat. Med.,* **3,** 1089–1095.

HARA, Y., WAKAMORI, M., ISHII, M., MAENO, E., NISHIDA, M., YOSHIDA, T., YAMADA, H., SHIMIZU, S., MORI, E., KUDOH, J., SHIMIZU, N., KUROSE, H., OKADA, Y., IMOTO, K. & MORI, Y. (2002). LTRPC2 Ca^{2+}-permeable channel activated by changes in redox status confers susceptibility to cell death. *Mol. Cell,* **9,** 163–173.

HEINER, I., EISFELD, J. & LUCKHOFF, A. (2003). Role and regulation of TRP channels in neutrophil granulocytes. *Cell Calcium,* **33,** 533–540.

INAMURA, K., SANO, Y., MOCHIZUKI, S., YOKOI, H., MIYAKE, A., NOZAWA, K., KITADA, C., MATSUSHIME, H. & FURUICHI, K. (2003). Response to ADP-ribose by activation of TRPM2 in the CRI-G1 insulinoma cell line. *J. Membr. Biol.,* **191,** 201–207.

KOURIE, J.I. (1998). Interaction of reactive oxygen species with ion transport mechanisms. *Am. J. Physiol.,* **275,** C1–C24.

KRAFT, R., GRIMM, C., GROSSE, K., HOFFMANN, A., SAUERBRUCH, S., KETTENMANN, H., SCHULTZ, G. & HARTENECK, C. (2004). Hydrogen peroxide and ADP-ribose induce TRPM2-mediated calcium influx and cation currents in microglia. *Am. J. Physiol. Cell Physiol.,* **286,** C129–C137.

LUBISCH, W., GRANDEL, R., KOCK, M., MUELLER, R., HOEGER, T. & SCHULT, S. (2001). New azepinoindole derivatives are PARP inhibitors – useful for the treatment of e.g. stroke, Alzheimer's, Parkinson's or Huntington's disease, epilepsy, kidney damage, acute myocardial infarction, tumors, tumor metastasis, sepsis and ARDS. (DE10039610-A1), Patent.

MCHUGH, D., FLEMMING, R., XU, S.Z., PERRAUD, A.L. & BEECH, D.J. (2003). Critical intracellular Ca^{2+} dependence of transient receptor potential melastatin 2 (TRPM2) cation channel activation. *J. Biol. Chem.,* **278,** 11002–11006.

NAGAMINE, K., KUDOH, J., MINOSHIMA, S., KAWASAKI, K., ASAKAWA, S., ITO, F. & SHIMIZU, N. (1998). Molecular cloning of a novel putative Ca^{2+} channel protein (Trpc7) highly expressed in brain. *Genomics,* **54,** 124–131.

OLIVER, F.J., MENISSIER-DE MURCIA, J., NACCI, C., DECKER, P., ANDRIANTSITOHAINA, R., MULLER, S., DE LA, R.G., STOCLET, J.C. & DE MURCIA, G. (1999). Resistance to endotoxic shock as a consequence of defective NF-kB activation in poly (ADP-ribose) polymerase-1 deficient mice. *EMBO J.,* **18,** 4446–4454.

PERRAUD, A.L., FLEIG, A., DUNN, C.A., BAGLEY, L.A., LAUNAY, P., SCHMITZ, C., STOKES, A.J., ZHU, Q., BESSMAN, M.J., PENNER, R., KINET, J.P. & SCHARENBERG, A.M. (2001). ADP-ribose gating of the calcium-permeable LTRPC2 channel revealed by Nudix motif homology. *Nature,* **411,** 595–599.

SANO, Y., INAMURA, K., MIYAKE, A., MOCHIZUKI, S., YOKOI, H., MATSUSHIME, H. & FURUICHI, K. (2001). Immunocyte Ca^{2+} influx system mediated by LTRPC2. *Science,* **293,** 1327–1330.

SKAPER, S.D. (2003). Poly(ADP-ribosyl)ation enzyme-1 as a target for neuroprotection in acute central nervous system injury. *Curr. Drug Target CNS Neurol. Disord.,* **2,** 279–291.

SMITH, S. (2001). The world according to PARP. *Trends Biochem. Sci.,* **26,** 174–179.

SUAREZ-PINZON, W.L., MABLEY, J.G., POWER, R., SZABO, C. & RABINOVITCH, A. (2003). Poly (ADP-ribose) polymerase inhibition prevents spontaneous and recurrent autoimmune diabetes in NOD mice by inducing apoptosis of islet-infiltrating leukocytes. *Diabetes,* **52,** 1683–1688.

TAKAHASHI, K., GREENBERG, J.H., JACKSON, P., MACLIN, K. & ZHANG, J. (1997). Neuroprotective effects of inhibiting poly(ADP-ribose) synthetase on focal cerebral ischemia in rats. *J. Cereb. Blood Flow Metab.,* **17,** 1137–1142.

TANUMA, S., YAGI, T. & JOHNSON, G.S. (1985). Endogenous ADP ribosylation of high mobility group proteins 1 and 2 and histone H1 following DNA damage in intact cells. *Arch. Biochem. Biophys.,* **237,** 38–42.

VARANI, J., PHAN, S.H., GIBBS, D.F., RYAN, U.S. & WARD, P.A. (1990). H_2O_2-mediated cytotoxicity of rat pulmonary endothelial cells. Changes in adenosine triphosphate and purine products and effects of protective interventions. *Lab. Invest.,* **63,** 683–689.

VIRAG, L. & SZABO, C. (2002). The therapeutic potential of poly(ADP-Ribose) polymerase inhibitors. *Pharmacol. Rev.,* **54,** 375–429.

WEHAGE, E., EISFELD, J., HEINER, I., JUNGLING, E., ZITT, C. & LUCKHOFF, A. (2002). Activation of the cation channel long transient receptor potential channel 2 (LTRPC2) by hydrogen peroxide. A splice variant reveals a mode of activation independent of ADP-ribose. *J. Biol. Chem.,* **277,** 23150–23156.

ZHANG, W., CHU, X., TONG, Q., CHEUNG, J.Y., CONRAD, K., MASKER, K. & MILLER, B.A. (2003). A novel TRPM2 isoform inhibits calcium influx and susceptibility to cell death. *J. Biol. Chem.,* **278,** 16222–16229.

(Received February 9, 2004
Revised April 22, 2004
Accepted June 11, 2004)